A DSP-Based Lane Departure Warning System

Bing-Fei Wu, Chao-Jung Chen, Yi-Pin Hsu and Ming-Wei Chung
Department of Electrical and Control Engineering
National Chiao-Tung University
1001 Ta-Hsueh Road, Hsinchu
Taiwan R.O.C.

Abstract: - A DSP-Based adaptive lane departure warning system (ALDWS) is presented in this paper. The system can be applied in highways, tunnels and urban roadways, and works well in sunny, cloudy, and rainy conditions in day or night. Different types of lane markings can be detected, such as solid, dashed, double, etc., by the proposed vision-based detection algorithm. The DSP image processor on ALDWS works with operating frequency of 600MHz and the lane marking detection speed can be more than 35 frames per second with QVGA size. The presented fast adaptive lane detection algorithm is efficient and robust at both day and night. A modified lane model is proposed to increase the accuracy of detection. Moreover, an automatic calibration between the lane width and the road inclination is considered and adjusted on-line. ALDWS is equipped on the smart car, TAIWAN *i*TS-1, and has been successfully verified for hundreds of kilometers on Highway No.3 and Expressway No.68 in Taiwan.

Key-Words: - Lane departure warning, vision-based detection

1 Introduction

In recent years, traffic accidents stand at the rock-solid fifth rank of the first ten causes of death in Taiwan, i.e. thousands of people were dead or injured in these accidents. In 2005, there were over 2700 motor vehicle crashes occur involving fatalities, where 2894 people were killed [1].

Recently the U.S. National Highway Transportation Safety Administration (NHTSA) estimated that as many as 1,575,000 accidents annually are caused by distracted drivers; a large percentage of these accidents involve unintended lane departures. The U.S. government identifies lane departures as a major cause of rollover incidents involving sport utility vehicles and light trucks. According to NHTSA, 95% of single vehicle rollover accidents are "tripped" rollovers that occur when a vehicle leaves the roadway and slides sideways into the soft soil on the shoulder of the road or hits an object such as a curb or guardrail [2].

Some approaches are forced including the seat belts, air bags, heavy penalties for the driving against traffic regulations or rumble strips installation on the roadway to protect the drivers and passengers from the fatalities. However, these actions belong to passive protection strategies. Actually, the prior prevention of crashes is much more efficiently than the protection after crashing, i.e. the active protections deserve to be promoted in advanced safety vehicles, including lane departure warning system, blind spot monitoring, rear view collision avoidance, etc. In this paper, an adaptive lane departure warning system (ALDWS) is presented to assist drivers avoiding run-off-road and sides swipe collisions.

For lane departure warning approach, the lane boundaries ahead of the vehicle and the vehicle's position within the lane are the key information for lane departure warning decision. Several sensing technologies have been investigated for lane detection and position estimation studies; e.g. embedded magnetic markers in the roadway, highly accurate Global Position System (GPS) with digital maps, infrared sensors, image processing, etc.

In U.S.A., a famous PATH program demonstrated an infrastructure-based approach, which embedded the specified magnetic markers in the roadway to form the traveling path information and the magnetometer mounted on the front of vehicles received it. This is a highly reliable solution; however, it suffers from high cost and huge infrastructure requirement [3].

Another approach is to combine GPS and digital maps to achieve lane tracking. The IV Lab. at the University of Minnesota applied differential GPS information and high resolution digital maps to determine lane position [4, 5]. This kind of systems work in all weather conditions e.g. bright sun, rain, snow, fog, etc. However, GPS drops out from bridges and other objects those may affect the availability. In addition the highly detailed maps are required and those must be continuously updated [6].

In European market, the infrared-based LDWS for several current models has been announced to warm the driver of the unintended lane departure. When the vehicle moves across road markings without permission, e.g. turn signals, the driver will be warned by means of a vibrating signal on the left or right side of the driver's seat, depending which way the vehicle is drifting [7]. This LDWS uses six infrared sensors which are mounted under the front bumper of the vehicle, three on each side, to identify lane markings on the roadway. Each sensor is equipped with an infrared light-emitting diode and a detection cell. The departures are detected by variations in the reflections from the infrared beams emitted by the diode onto the road.

In the decade, many vision-based LDWSs are presented based on the robust lane marking/boundary detection and vehicle position estimation algorithms. The projection model from 3D world coordinate to 2D image plane is first addressed in [8, 9]. The parabolic models have been proposed to approximate lane geometry. In [10-13], the inverse perspective mapping is utilized to obtain a bird's eye-view image for lane extraction. Several researches [14-18] used deformable road models to fit the lane boundaries. The principle, prediction-verification-updating, is popularly utilized in these systems for real-time updating some parameters in the models [8, 9], especially in the various roadway conditions and the vehicle's vibrating and suspension.

The main purpose of this investigation is to implement a real-time lane detection algorithm and the vehicle position within the lane on the DSP-based image processor (DSPIP). This algorithm is also a prediction-verification-updating one with the modified model from 3D coordinate to image plane. ALDWS detects lane markings on the road and estimates the vehicle's position within its lane by using a monochromatic CCD camera with a 6mm lens in Fig. 1. The CCD is mounted behind the windshield on the experimental smart car, TAIWAN *i*TS-1, as shown in Fig. 2.

Fig. 1 The monochromatic CCD mounted behind the windshield

Fig. 2 TAIWAN *i*TS-1

This paper is organized as follows. Section 2 states the lane detection and position estimation. The experimental results are addressed in Section 3. Section 4 gives the conclusions and future work.

2 Detection and Estimation Algorithm

Lane detection and position estimation are the two key functions of ALDWS. The proposed lane detection algorithm uses a two-stage process to enhance the efficiency. The first stage is for images where no previous information of lane marking pixels and lane trends exists. The second one works on the images when the lane marking pixels and lane trends are detected in the previous stage. When it appears that the lane cannot be successfully identified, the first stage runs again. The first stage is a full range search of the selected area. The detected lane marking pixels are approached to a second order polynomial and its curvature on image plane is taken as the lane trend information. In the second detection stage, the search area is smaller than the one in the first stage because the detected lane information in the first stage is available for reference.

2.1 Coordinate Transformation

Initially during detection, the point in global coordinates (*x, y, z*) are projected onto the image plane (*u, v*), as shown in Fig. 3. The projection plane with respect to global coordinates can be obtained by

$$u = e_u \frac{x}{y} \tag{1}$$

and $$v = e_v \frac{z - H}{y}, \tag{2}$$

where $e_u = f/du$ and $e_v = f/dv$ with the physical width and height of an image pixel, *du* and *dv*. The parabolic polynomial lane model is utilized in the proposed algorithm, as given by

$$x = k \cdot y^2 + m \cdot y + b\,. \tag{3}$$

From (1) and (2), (4) and (5) are illustrated, where $z = m_\theta \cdot y$.

$$x = \frac{u \cdot H}{e_v \cdot m_\theta - v} \cdot \frac{e_v}{e_u} \tag{4}$$

and $$y = e_v \frac{H}{e_v \cdot m_\theta - v} \tag{5}$$

By substituting (4) and (5) into (3), one yields

$$u = \frac{k e_u e_v H}{e_v m_\theta - v} + m e_u + \frac{b e_u}{H e_v}(e_v m_\theta - v) \tag{6}$$

to represent the lane model in terms of image coordinates (u, v) with a road inclination m_θ.

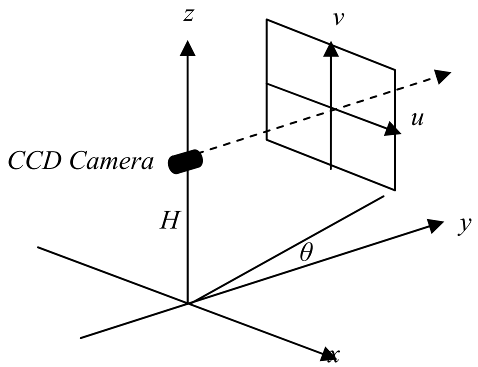

Fig. 3. The relationship between world space and image plane.

In another point, $P_i(x_i, y_i, z_i)$ is the coordinate of some lane position in world space and $i \in \{L, M, R\}$, where L, M and R denote the left, middle and right sides of the lane. The middle point of the lane, P_M, is defined as $P_M = (P_L + P_R)/2$. On the image plane, the coordinate, (u_i, v_i), indicates the lane position. From (1) and (2), we have

$$\frac{1}{2}(u_R + u_L) = u_M = e_u \frac{x_M}{y_M}, \tag{7}$$

$$(u_R - u_L) = e_u \frac{x_R - x_L}{y_M} = e_u \frac{W}{y_M} \tag{8}$$

and $$v_R = v_L = v_M = e_v \frac{z_M - H}{y_M}, \tag{9}$$

where W denotes the lane width. x_M, y_M and z_M are obtained from (7), (8) and(9),and determined as

$$x_M = \frac{u_M \cdot W}{u_R - u_L} \tag{10}$$

$$y_M = e_u \frac{W}{u_R - u_L}. \tag{11}$$

$$z_M = H + \frac{v_M \cdot W}{u_R - u_L} \cdot \frac{e_u}{e_v}. \tag{12}$$

By substituting (10) and (11) into (3), it yields

$$u_M(u_R - u_L) = k e_u^2 W + m e_u (u_R - u_L) + \frac{b}{W}(u_R - u_L)^2 \tag{13}$$

Both (6) and (13) represent the lane model in image coordinates, (6) is available if m_θ is given and (13) is formed based on the assumption that W is a given constant. (6) and (13) are combined together in our algorithm to predict k, m, and b parameters in (3). With the given detected lane marking pairs, (u_L, u_R), the terms of (13) are determined by weighted least square approximation so that k, m, and b parameters are evaluated.

2.2 Lane Detection Algorithm

The proposed lane detection algorithm on ALDWS follows prediction-verification-updating principle [8, 9]. In the prediction part, a first-order Taylor polynomial is utilized to estimate the next candidate of the lane marking position according to the deficient previous detected information. Once the previous detected lane marking points are sufficient, the least square approximation is instead of the first-order Taylor polynomial. Not only the position estimation, but also the region of interesting of detection for the next lane marking is also defined.

The intensity of the lane markings is applied with its dark-light-dark (DLD) characteristic, as shown in Fig. 4(a). A point M is located at the DLD transmission if the intensity of M, I_M, exceeds that of its left and right side neighbors by half of lane marking width on image plane, $MI/2$, as shown in Fig. 4 (b). The points L and R are defined if L and R own the maximum gradients in the $[M - MI/2, M)$ and $(M, M + MI/2]$ intervals, respectively, in Fig. 4(c). Once L and R are picked, $\overline{LR}$ is taken as lane marking in Fig. 4 (d) if $\overline{LR} > \overline{LR}_{th}$, where $\overline{LR_{th}}$ is a predefined threshold. Note that R of the left hand $\overline{LR}$ is chosen as the marking coordinate and L of the right hand $\overline{LR}$ stands for the one. The lane markings are searched zone by zone, while the zone is scanned row by row, from bottom to top, as illustrated in Fig. 5. When some zone completes the lane marking detection, the lane tendency is approximated by those detected lane marking information for the next zone since the previous lane tendency deserved to be referred. The least square method is applied for the approximation.

The parameters, m_θ and W, are on-line automatic calibrated after per ten processed images. We use the $z = \tan\theta \cdot y$ definition of z axis in world space and replace z and y from (11) and (12) to obtain

$$v_M = C_{zy0} - C_{zy1} \cdot \Delta u \ , \tag{14}$$

where $C_{zy0}=e_v \cdot m_\theta$ and $C_{zy1}=e_v H/e_u W$. The weighted least square method yields the coefficients C_{zy0} and C_{zy1} in (14) and afterward m_θ and W are available by the inverse calculation. The lateral offset, $O(y)$, is according to the coefficients in (3), k, m, and b, by

$$O(y) = k \cdot y^2 + m \cdot y + b \ , \tag{15}$$

where y is set as the desired distance ahead the vehicle.

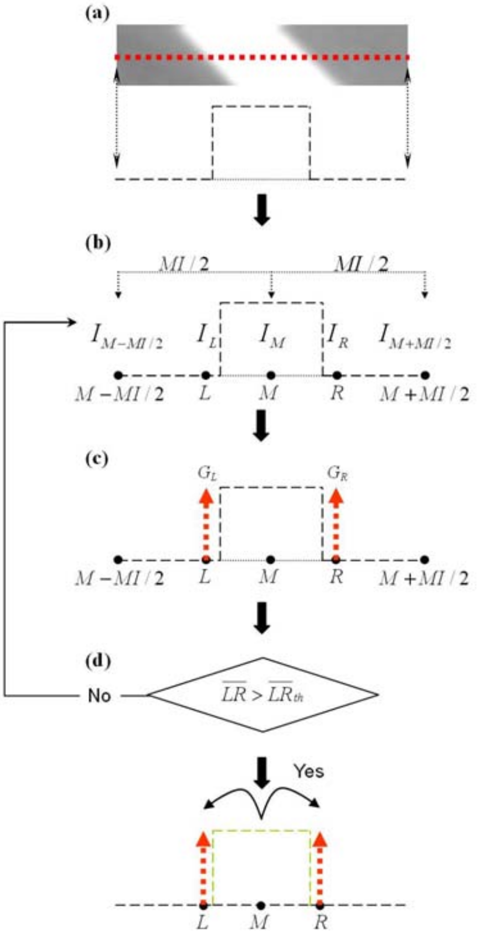

Fig. 4 Lane marking detection

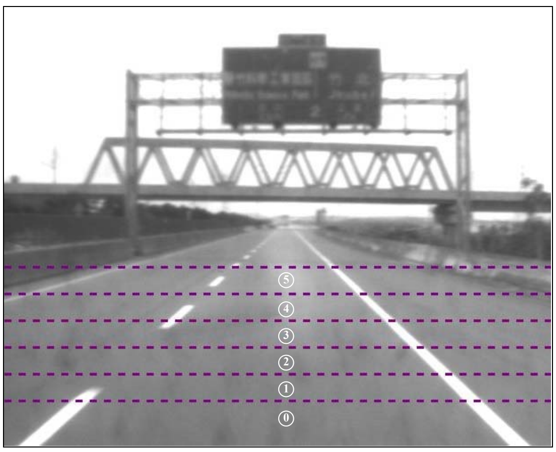

Fig. 5 The detection zone division

2.3 Position Estimation

The CCD of ALDWS is arranged in the center behind the windshield, so that the center line on the image is sufficient to indicate the one of the vehicle, as shown in Fig. 6. The lateral offset is defined in (15), where *k, m, b* are given from the proposed algorithm, and then calculate the offset with the desired distance, y. Note that, the distance is from the CCD to the desired point, instead of that from the head of the vehicle.

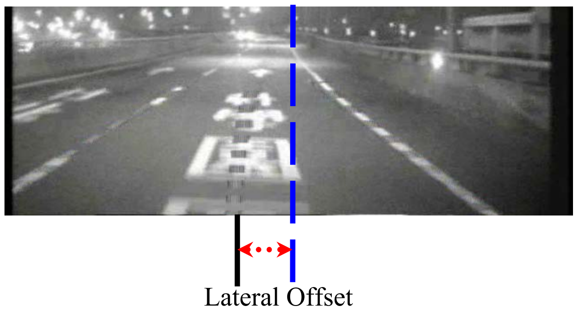

Fig. 6 The lateral offset definition

3 Experimental Results

The raw data of an image from the camera is sent to DSPIP for real-time recognition. The recognition speed can achieve more than 35 frames per second with QVGA size. This system works well in sunny, cloudy, and rainy weather conditions in day or night. Different types of lane markings can be detected, such as solid, dashed, double, yellow, etc. ALDWS is qualified for highway, urban, and tunnel applications at all vehicle speeds.

ALDWS is equipped on our experimental car, TAIWAN *i*TS-1, and has real-road verified for hundreds of kilometers. ALDWS performs well even with poor roadway markings and conditions, such as strong shadows, text on the road, harsh lighting, reflected light from the road surface and other vehicles. Fig. 7 shows the detection results for these difficult conditions. Figure 7(a) is the result in urban area and Fig. 7(b) to Fig. 7(f) are the ones on highway and expressway.

ALDWS also works well inside tunnels and under heavy rains, as shown in Fig. 8. In rainy cases, ALDWS overcomes the influences of wipers and water drops on the windshield. When it appears that the vehicle intends to depart from its lane, as shown in Fig. 9(b) and Fig. 9(d), visual and audible warning signals alert the driver to take corrective driving. As shown in Fig. 9(a) and Fig. 9(c), the alarm signals were disabled since TAIWAN *i*TS-1 keeps stable in the lane. The visual alarm enables since the turn signal is un-triggered.

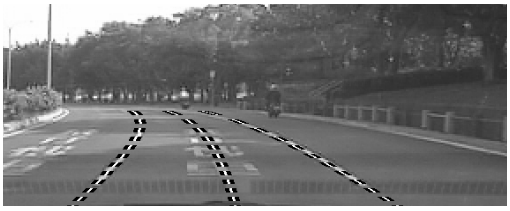
(a) Text on the road at daytime


(b) Curve lane with sufficient lighting


(c) Dim lighting condition


(d) Insufficient lighting condition


(e) Curve lane under seriously insufficient lighting


(f) Reflected lights from road surface and the taillight of the previous vehicle

Fig. 7 The detection results of difficult road conditions


(a) Rainy day condition


(b) Rainy day condition with wiper interference


(c) Rainy night condition with the water drops on the windshield


(d) Rainy night condition with harsh lighting

Fig. 8 The detection results under rainy condition


(a) Stable in the lane


(b) Departure from the lane


(c) Stable in the lane

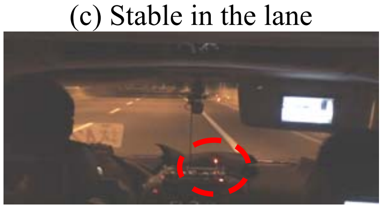
(d) Departure from the lane

Fig. 9 The visual alerts to the drivers when departure appears

4 Conclusions

ALDWS based on a DSPIP has been successfully implemented to serve drivers for their unintentional lane departure. It is also equipped on TAIWAN *i*TS-1 for hundreds of kilometers verification on Highway No. 3 and Expressway No. 68 in Taiwan. The proposed lane detection algorithm works well under different weather conditions in day and night. Different types of lane marking in straight or curve lanes won't influence the performance of departure warning. Future work will concentrate on studying the vision-based vehicle detection and distance estimation to warn the drivers when the vehicle and the previous car are too close. Certainly, this will be integrated on the DSPIP to extend the functions of ALDWS.

References:

[1] http://www.moi.gov.tw/stat/english/index.asp

[2] M. Fitzgerald, "Lane Departure Warning boots Anti-Rollover Protection", Strategy Analytics in Automotive DesignLine, http://www.automotivedesignline.com/howto/60405845

[3] R. Rajamani, T. Han-Shue, L. Boon Kait, Z. Wei-Bin, "Demonstration of integrated longitudinal and lateral control for the operation of automated vehicles in platoons", IEEE Trans. Control Systems Technology, vol. 8, pp.695-708, July, 2000.

[4] B. Richard, "Intelligent Vehicle Technology and Trends", pp. 99

[5] M. Donath, "The Vehicle-Highway Partnership:The Infrastructure Needs to Get Smarter," ITS Institute, University of Minnesota, *Proceedings of the 7th International Task Force on Vehicle-highway Automation*, Paris, 2003.

[6] http://www.IVsource.net

[7] http://www.citroen.com/CWW/en-US/TECHNOLOGIES/SECURITY/AFIL/

[8] R. Chapuis, J. Gallice, F. Jurie, and J. Alizon, "Real time road mark following", *Signal Processing*, vol. 24, pp. 331-343, Dec. 1991.

[9] R. Chapuis, R. Aufrere, and F. Chausse, "Accurate road following and reconstruction by computer vision," *IEEE Trans. Intelligent Transport. Systems*, vol. 3, pp. 261-270, Dec. 2002.

[10] A. Broggi, M. Bertozzi, Lo Guarino, C. Bianco, and A. Piazzi, "Visual perception of obstacle and vehicles for platooning," *IEEE Trans. Intelligent Transport. Syst.*, vol. 1, no. 3, pp. 164-176, Sept. 2000.

[11] M. Bertozzi and A. Broggi, and A. Fascioli, "Obstacle and lane detection on ARGO autonomous vehicle," in Proc. *IEEE Intelligent Transportation System Conf.* '97, Boston, MA. pp. 1010-1015.

[12] M. Bertozzi and A. Broggi, "GOLD: A parallel real-time stereo vision system for generic obstacle and lane detection," *IEEE Trans. on Image Processing*, vol. 7, pp. 62-81, Jan. 1998.

[13] M. Bertozzi and A. Broggi, "Vision-Based Vehicle Guidance," *Computer*, vol. 30, pp. 49-55, July. 1997.

[14] Y. Wang, D. Shen, and E. Teoh, "Lane detection using catmullrom pline," *in Proceedings of IEEE Intelligent Vehicles Symposium*, Stuttgart, Germany, 1998, pp. 51–57.

[15] J. Goldbeck and B. Huertgen, "Lane detection and tracking by video sensors," in *Proceedings of IEEE Intelligent Transportation Systems*, vol. 1, October 1999, pp. 74–79.

[16] R. Risack, N. Mohler, and W. Enkelmann, "A video-based lane keeping assistant," in *Proceedings of IEEE Intelligent Vehicles Symposium*, Dearborn, MI, October 2000, pp. 506–511.

[17] J. Park, J. Lee, and K. Jhang, "A lane-curve detection based on an LCF," *Pattern Recognition Letters*, vol. 24, no. 14, pp. 2301–2313, October 2003.

[18] Y. Wang, E. Teoh, and D. Shen, "Lane detection and tracking using B-snake," *Image and Vision Computing*, vol. 22, no. 4, pp. 269–280, April 2004.